HHS Public Access

Author manuscript

Biofabrication. Author manuscript; available in PMC 2019 June 29.

Published in final edited form as:

Biofabrication. ; 10(3): 034106. doi:10.1088/1758-5090/aacdc7.

Optimization of gelatin-alginate composite bioink printability using rheological parameters: a systematic approach

Teng Gao[1,†], **Gregory J. Gillispie**[1,2,†], **Joshua S. Copus**[1,2], **Anil Kumar Pallickaveedu Rajan Asari**[1], **Young-Joon Seol**[1], **Anthony Atala**[1,2], **James J. Yoo**[1,2], and **Sang Jin Lee**[1,2,*]

[1]Wake Forest Institute for Regenerative Medicine, Wake Forest School of Medicine, Winston-Salem, North Carolina, USA

[2]School of Biomedical Engineering and Sciences, Wake Forest University-Virginia Tech, Winston-Salem, North Carolina, USA

Abstract

Three-dimensional (3D) bioprinting has emerged as a promising technique in tissue engineering applications through the precise deposition of cells and biomaterials in a layer-by-layer fashion. However, the limited availability of hydrogel bioinks is frequently cited as a major issue for the advancement of cell-based extrusion bioprinting technologies. It is well known that highly viscous materials maintain their structure better, but also have decreased cell viability due to the higher forces which are required for extrusion. However, little is known about the effect of the two distinct components of dynamic modulus of viscoelastic materials, storage modulus (G') and loss modulus (G''), on the printability of hydrogel-based bioinks. Additionally, "printability" has been poorly defined in the literature, mostly consisting of gross qualitative measures which do not allow for direct comparison of bioinks. This study developed a framework for evaluating printability and investigated the effect of dynamic modulus, including storage modulus (G'), loss modulus (G''), and loss tangent (G''/G') on the printing outcome. Gelatin and alginate as model hydrogels were mixed at various concentrations to obtain hydrogel formulations with a wide range of storage and loss moduli. These formulations were then evaluated for the quantitatively defined values of extrudability, extrusion uniformity, and structural integrity. For extrudability, increasing either the loss or storage modulus increased the pressure required to extrude the bioink. A mathematical model relating the G' and G'' to the required extrusion pressure was derived based on the data. A lower loss tangent was correlated with increased structural integrity while a higher loss tangent correlated with increased extrusion uniformity. Gelatin-alginate composite hydrogels with a loss tangent in the range of 0.25 to 0.45 exhibited an excellent compromise between structural integrity and extrusion uniformity. In addition to the characterization of a common bioink, the methodology introduced in this paper could also be used to evaluate the printability of other bioinks in the future.

*Corresponding author: Sang Jin Lee, PhD, Medical Center Boulevard, Winston-Salem, NC 27157, USA, Tel: 1-336-713-7288, sjlee@wakehealth.edu.

†Equal contribution

Keywords

dynamic modulus; viscoelasticity; hydrogel; bioink; bioprinting; tissue engineering

1. Introduction

Over the last decade, exciting advances in tissue engineering and regenerative medicine have been made through three-dimensional (3D) bioprinting technologies (1–4). Precise deposition through microextrusion of cell-laden hydrogels in a layer-by-layer fashion has allowed fabrication of complex, composite tissue and organ structures (5–8). However, a crucial yet limiting aspect of current bioprinting modalities is the availability of bioink materials (2, 9, 10). The ideal bioinks for cell-based microextrusion printing should fulfill three major requirements: (i) relatively higher viscosity, (ii) strong shear-thinning behavior, and (iii) rapid crosslinking process after printing (2). Due to the inability of most hydrogels to be self-supporting upon layer-by-layer deposition, nearly all bioink systems require second-stage crosslinking directly after printing (11–14). Open microchannels inside a printed tissue construct play a crucial role in cell survival and function for a variety of tissue types by facilitating oxygen transfer, deliver nutrients, and the removal of metabolic waste (5, 15). The fabrication of multi-layered porous structures requires both a high printing shape fidelity during the printing process and the prevention of collapsing or sagging after printing (1). Simultaneous printing of hydrogel-based bioinks with supporting and sacrificial materials like poly(ε-caprolactone) (PCL) and Pluronic F127, respectively, is one of the approaches to circumvent these limitations (5). However, the slow degradation and high stiffness of polymeric materials will pose restrictions on this approach, especially for soft tissue fabrication (13). Therefore, a single optimized printable bioink material or formulation with appropriate rheological, biomechanical, and biological properties is highly desirable.

Several sets of criteria for bioink properties have been proposed in the past (9, 11, 16–19). Although informative, most of these criteria were broad requirements for the material to fulfill rather than practical engineering specifications and guidelines. When designing a bioink, one of the most important considerations is rheology (20). Surprisingly, the role of rheology in bioink formulations remains poorly understood and many studies do not take rheology into consideration during bioink development and evaluation. The vast majority of rheological characterizations of bioinks have focused on hydrogel viscosity (11). Bioink viscosity can directly impact both printing shape fidelity and printing pressure necessary to dispense the material, which in turn can affect cell viability; however, viscosity alone cannot capture the complex behavior of hydrogel-based bioinks during the printing process (21, 22).

Bioink viscosity has been reported as the determining factor of printing shape fidelity (9); however, high viscosity does not necessarily confer high mechanical strength or printing accuracy (e.g. low concentration hyaluronic acid) (10). This is due to two distinct components of dynamic modulus : storage modulus (G') and loss modulus (G''), as shown in Eq. (1). To date, viscosity has been thought of as a single parameter when determining the proper composition of a bioink. Most studies have focused on reporting the G' component

of viscosity for a particular type of hydrogel being developed and the role of G'' is largely ignored (13, 14, 17). In Figure 1A, the ratio between G' and G'' determines if a material is solid-like or liquid-like. The ratio of G'' to G' is defined as the loss tangent (tanδ), shown in Eq. (2), where δ is the phase angle of the material. Little is known about the effect of these two rheological parameters and their respective ratio (loss tangent) on the printing outcome.

$$\eta* = \frac{(G'^2 + G''^2)^{1/2}}{\gamma'} \quad (1)$$

$$tan\delta = \frac{G''}{G'} \quad (2)$$

Highly viscous hydrogels, with appropriate ratios between G' and G'', are desirable to achieve a good printing resolution with sufficient mechanical strength for maintaining structural integrity (9). However, materials with a higher viscosity require higher extrusion forces. This can lead to higher shear stresses experienced by the cells and result in severe cell damage (13). Studies have shown that exposure to high levels of shear stress during the printing process can affect both immediate and long-term cell viability and proliferation (21). A quantitative relationship between nozzle size and dispensing pressure on cell viability has been found (23). Hence, another important criterion for a printable hydrogel is its extrudability: the dispensing pressure needed to achieve extrusion at a sufficient flow rate (or print head speed). Due to the different sensitivity of different cell types, controlling the shear stress during the extrusion pressure is of critical importance for cell-based bioprinting. To date, a quantitative correlation has not been established between storage and loss moduli and required extrusion pressure. Moreover, a standard method to evaluate the bioink printability does not yet exist (20).

In this study, the main objective was to investigate the effect of material loss (G'') and storage moduli (G') and their respective ratio (tanδ) on the printability of gelatin-alginate composite hydrogels, a common bioink used in bioprinting. In addition, experimental methods for the quantification of bioink printability were developed using extrudability, extrusion uniformity, and structural integrity as the defining parameters.

2. Materials and Methods

2.1. Bioprinting system

The integrated tissue-organ printer (ITOP) and motion program previously developed by our laboratory were used (5). Briefly, the ITOP is composed of an XYZ stage/controller, dispensing module, and a closed chamber. A three-axis stage system having 200 × 200 × 100 mm^3 travel and controller were used to provide printing paths for printing process (Aerotech, Inc., Pittsburgh, PA). The dispensing module consisted of a precision pneumatic pressure controller, syringe, and Teflon nozzle (Musashi Engineering, Inc., Tokyo, Japan).

Finally, the closed-chamber system was constructed by equipping a temperature controller (EIC Solutions, Inc., Warminster, PA) in the customized acrylic enclosure. The printing pattern, scan speed, extrusion pressure, and dispensing materials were specified in a custom text-based motion program. This motion program was then transferred to the operating computer for printing 3D structures.

2.2. Hydrogel bioink preparation

Sodium alginate and gelatin (type A, 90–110 bloom derived from porcine skin) were purchased from Sigma Aldrich (St. Louis, MO). Bioink formulations were prepared with various ratios of alginate and gelatin. Briefly, gelatin was first dissolved in Dulbecco's Modified Eagle Medium (DMEM, Gibco, Thermo Fisher, Waltham, MA) on a rotational shaker at 37°C for 60 min. Sodium alginate was then added to gelatin solution, and gelatin-alginate mixtures with different ratios were mixed on a rotational shaker at 37°C for additional 3 h. Afterward, all bioink formations were kept at room temperature (23–24°C) for 4–10 h prior to rheological tests. All subsequent experiments were conducted at room temperature.

2.3. Rheological measurement

Rheological measurements of bioink formulations were performed with a Discovery Hybrid Rheometer-2 (TA Instruments, Newcastle, DE) with a steel 8-mm parallel plate geometry at room temperature. Custom molds (made by MakerBot Replicator 2X, New York, NY) containing each bioink sample were immobilized on the Peltier plate using double-sided tape. Subsequently, the steel plate geometry was lowered until contact with the surface of the bioink sample. For solid phase gels ($G' > G''$), the geometry was lowered further until the axial force on the instrument equaled 0.02 N. For liquid phase gels, geometry was lowered until contact with the surface. After contact, the shear elastic modulus G', shear loss modulus G'', and loss tangent tan(δ) were measured for each hydrogel bioink using a shear strain sweep test ranging from 0.02% to 1.0% at an oscillation frequency of 1 Hz (12). All rheological measurements were conducted in triplicate.

2.4. Printing extrudability

Extrudability was defined as the minimum pneumatic pressure to extrude the material at a set flow rate. A syringe containing the bioink sample was loaded onto the ITOP bioprinter. For all measurements, a 260-μm nozzle (Nordson EFD, East Providence, RI) was used. A one layer zig zag 10 × 10 mm^2 deposition pattern (scanning speed: 200 mm/min) was used for extrudability testing. For each sample, 3 different values of pneumatic pressure were applied and the weight of the extruded material was recorded 3 times at each level of pressure. The average extrudate weights at different levels of pressure were then plotted against the pressure values. Due to the non-Newtonian behavior of the hydrogel bioinks used in this experiment, a power law function was fitted to the data points (24). Using this function, the extrusion pressure at 100 mg extrudate weight was extrapolated for each bioink formulation. The specific weight was chosen for continuous extrusion and to minimize variability in flow rate for all bioink formulations.

2.5. Extrusion uniformity

For each bioink formulation, 3 filaments were extruded according to the conditions in Table 1. To control for the flow rate of different hydrogel formulations, the pressure was adjusted until the weight of the extrusion lines was equal for each test. Photographic images were taken from each print and analyzed in ImageJ software. The uniformity of each filament was measured by manually outlining the hydrogel on both sides of the extrusion line and measuring the length in pixels. This value was then divided by what the length in pixels of a perfectly uniform gel would have been, i.e. a straight line on each side. This value was defined as the 'uniformity ratio' (Figure 3A).

2.6. Structural integrity

5-layer cylindrical structures (diameter: 12 mm) were printed using the ITOP system. The layer height was specified as 0.38 mm and a 25G nozzle was used. Silicone elastomer was used as a control to offset any magnification error in imaging and deviation from the programmed shape caused by the printing process. Approximately 30 mg of materials were extruded for each bioink formulation. High-resolution pictures were taken by a Dino-Lite digital microscope (AnMo Electronics Co., Taiwan) under the same light condition, and the height of the build structures was measured by ImageJ software. Bioprinting structural integrity of the hydrogel formulations was quantified by comparing the measured height of the bioink samples to the measured height of the control.

2.8. Statistical analysis

Statistical analyses were performed using JMP 13 (SAS Institute Inc., Cary, NC). Comparisons between different bioink formulations were done using a one-way analysis of variance (ANOVA) with a significance level of $p < 0.05$. If significance was reached, differences were identified using Tukey's *post-hoc* test, also with a significance level of $p < 0.05$.

3. Results

3.1. Rheological properties of gelatin-alginate bioinks

Rheological characteristics of two common bioink materials, gelatin and alginate, used in this study were measured using a standard protocol. Each material with different concentrations was tested in order to observe the effect of hydrogel concentration on rheological properties. Figure 1A summarizes four general classes of naturally derived hydrogel materials based on their viscoelastic properties. The ideal bioink should be self-supporting and can be extruded through a thin nozzle. A comparison between the rheological properties of gelatin and alginate was made. Increasing the concentration of gelatin resulted in an increase in the storage modulus and overall viscosity, while the loss modulus of gelatin hydrogel was close to zero for all concentrations (Figure 1B). This suggests that the nature of the network formed by gelatin is highly elastic rather than viscous. Due to this characteristic, gelatin hydrogels can be classified as a stiff solid bioink material at room temperature, which may be not ideal for the extrusion-based printing method. On the other

hand, alginate hydrogels formed a liquid phase gel and had a high loss tangent consistent throughout different concentrations (Figure 1C) (21).

In order to establish a model which correlates G' and G'' of the bioink formulations to the printing outcomes, it is necessary to be able to adjust the two moduli independently. According to the measurements described above, no single material proved to be sufficient for this purpose. To combat this, mixtures of gelatin and alginate were used as the model materials since gelatin has the most solid-like characteristic (G' dominates) and alginate has the most liquid-like characteristic (G'' dominates). A synergetic effect was observed when gelatin was mixed with alginate: loss modulus was introduced into the material while the storage modulus of gelatin was further enhanced, as shown in Figure 1D. Increasing the alginate concentration led to an increase in loss modulus, while an increase in gelatin concentration led to an increase in storage modulus. Bioink formulations of the gelatin-alginate mixture were selected as the main experimental hydrogel due to their accessibility and complementary nature. Thus, bioinks with a wide spectrum of loss tangent values (= G'/G''), but with similar stiffness were able to be obtained, as shown in Figure 1E and 1F.

3.2. Printing extrudability

Viscosity is sometimes thought of as a single factor which affects the extrudability of a bioink, but in this study, both components of dynamic modulus, G' and G'', were investigated on a quantitative basis. In this approach, the storage modulus (G') and the loss modulus (G'') were assumed to be the two independent variables as predictors of the required extrusion pressure (P). A first-order interactive model with two independent variables can be expressed as in equation 3, where β_0, β_1, and β_2 are constants.

$$P = \beta_0 + (\beta_1 \times G') \times (\beta_2 \times G'') + (\beta_3 \times G' \times G'') \quad (3)$$

The resulting best-fit model is summarized in Figure 2B. The results show that the required extrusion pressure of a bioink is co-determined by G' and G''. Both independent variables are positively correlated to the required extrusion pressure (P). Although the overall trend is that P increases as complex viscosity increases, P grows more rapidly when G'' rises. One possible explanation is that during the extrusion process, the bioink experiences both low and high-frequency deformation. At a higher frequency, the viscous component of the gel exhibits more solid-like property. If bioink extrusion is a process where high-frequency deformation dominates, G'' will make a bigger contribution to the required extrusion pressure. The resulting predictive model can be expressed as:

$$P = 26.6 + (0.05 \times G') + (0.07 \times G'') - (0.0000035 \times G'' \times G'') \quad (4)$$

Interestingly, a significant drop in required extrusion pressure was observed when pure gelatin was mixed with alginate, as shown in Figure 2C.

3.3. Extrusion uniformity

The uniformity of filaments produced by the bioink samples with increasing loss tangent values was evaluated and summarized in Figure 3. At a low loss tangent value, the material produces a bumpy extrusion line. As loss tangent increased, so did the uniformity of the extrusion lines with a sharp transition occurring between the tan(δ) = 0.27 and tan(δ) = 0.43 hydrogels. Smooth, uniform extrusion lines were achieved for loss tangent values of 0.43 and higher.

3.4. Structural integrity

After printing 5-layer cylindrical structures, the loss tangent value of the bioink materials was found to be negatively related to its structural integrity. As loss tangent of the mixture increased, the printed structure began to collapse inwards and lose shape. This phenomenon confirms the hypothesis that loss modulus grants the material more flow character and will negatively impact bioprinting shape fidelity if its value is too high. Similar to the results for extrusion uniformity, the smoothness of the printed structure is compromised at low loss tangent values (Figure 4A).

4. Discussion

Naturally-derived hydrogel materials are commonly used as bioink materials in 3D bioprinting due to their biological and physical properties. However, their rheological properties are poorly documented and the viscosity of a bioink material is still occasionally regarded as a single parameter during bioink development. Currently, in the literature, there is also a lack of methodologies to quantitatively define printability for the evaluation of bioinks. This study first outlined a definition of printability which included the parameters extrudability, extrusion uniformity, and structural integrity. Rheological characterization was then conducted for two commonly used bioink materials: alginate and gelatin. The effect of their concentrations on storage modulus, loss modulus, and loss tangent was investigated first individually and then as a mixture. Next, it was established that storage modulus (G') and loss modulus (G'') have independent effects on the bioink extrudability, and a quantitative model was presented. Finally, gelatin-alginate composite bioinks with similar storage moduli, but varying loss tangents were evaluated for extrusion uniformity and structural integrity.

Summarizing the three criteria discussed above, it was concluded that when tanδ was approximately between 0.25 and 0.45, the gelatin-alginate composite bioinks could be printed with relatively good smoothness without compromising structural integrity. G' and G'' of the bioink could also predict the required extrusion pressure, which in turn is negatively related to cell viability. This optimal region is illustrated in Figure 5. This region is an approximation rather than an exact boundary. The bioinks outside of this boundary were still printable in a literal sense, but printability decreased the further the loss tangent is removed from this window. These boundaries may also be application dependent. For example, structural stability may be more important than extrusion uniformity (or vice versa) depending on the desired architecture. This is complicated further by other modifiable parameters which affect printing outcomes such as temperature, print head speed, nozzle

dimensions, and cell density (25). The effect of initial cell density on printability especially should be considered in future studies. Cheng et al. (26) found no change in rheological properties at a cell density of 10^7 cell/mL, but whether this holds true for printability itself and for various applications remains to be seen. These parameters were controlled for rather than varied in this study, but potentially could be adjusted accordingly to increase printability without changing the bioink. More research is still needed into the many factors which affect printability and their relationships to one another.

The results established in this study are consistent with observations in previous studies. A study reported that increasing proportions of alginate in a mixture of gelatin lead to unacceptable spreading upon deposition while a high gelatin concentration leads to impairment of the extrusion process due to increased viscosity (6). While the current study agrees with those findings, it also can suggest an alternative explanation. In Figure 1D, gelatin and alginate each contribute to the two distinct components of viscosity: storage modulus and loss modulus. The discontinuity during extrusion observed was a result of disproportionally high storage modulus rather than high complex viscosity (6). Additionally, the spreading upon deposition can be attributed to a disproportionally high loss modulus (6).

A limitation of this study is that only one model material was analyzed. While it is believed that a similar trend would be found within most hydrogels, further experimentation (Supplementary Data) found that the loss tangent ‘printability window’ (from 0.25 to 0.45) found in this study did not necessarily apply to all other bioinks. For example, 40% Pluronic F127 showed excellent extrusion uniformity despite having a near-zero loss tangent. There are many other rheological properties, such as yield stress (17, 27), which effect printability and must also be considered. Additionally, different materials have different degrees of shear-thinning and thixotropic properties. Their properties during the printing process and after printing are only estimated by the rheological measurement. Although a clear correlation was found for gelatin-alginate composite bioinks, it is possible there is an alternative explanation for the differential role in storage modulus and loss modulus and their effects on required dispensing pressure. For example, if the frequency and strain rate during extrusion were significantly different from what was rheologically tested, the values of G' and G'' could change under those conditions. However, rheological properties at a low frequency and strain rates offer more insight into the bioinks’ behavior after printing. Further study should include characterizations of the rheological properties of hydrogel formulations throughout a wide range of strain and frequency levels and incorporate the shear thinning and thixotropic index into the model (17, 22). Lastly, extrudability was used in this study as a direct proxy for cell viability, but the relationship between extrudability and cell viability is somewhat complex in nature. A more comprehensive system for the optimization of bioink printability should test cell viability directly.

Several other methods have been proposed in the literature to evaluate printability (17–19, 25, 27, 28) and until recently, most of these were only qualitative or semi-quantitative. In order to compare between bioinks and optimize for printability, more quantitative measures are needed. A common practice is to look at fiber formation (17, 19). By extruding a bioink into the air (as opposed to directly on the printing platform), several fiber types can be observed. Smooth, uniform fibers are desired, but bioinks with poor printability may instead

exhibit either droplet formation or irregular, fractured fibers. Layer stacking has also been proposed, where a grid pattern is printed and the patency and shape of the pores are observed (17, 18, 27, 28). Bioinks with poor printability may have their fibers fuse together or the pore shape will be irregular and deviate from the original design. In this study, these phenomena were quantified by the structural integrity and extrusion uniformity measurements. As more components of printability are identified and more methodologies for measuring those components are proposed, the disadvantages and advantages of each will need to be investigated. Ideally, a consensus definition for each component of 'printability' will eventually be reached, creating a standardization of evaluation methodologies, providing a framework for studying the factors which impact these phenomena and allowing for new bioinks to be developed more quickly and reliably.

5. Conclusions

This study established a quantitative approach to measure printability using extrudability, structural integrity, and extrusion uniformity. This was subsequently used to characterize and optimize gelatin-alginate composite bioinks. This study also demonstrated the impact loss modulus and loss tangent, two rheological properties often ignored in assessments of printability, can have on a bioink's performance. A quantitative model was established using mixtures of gelatin and alginate which highlighted the individual contributions of storage and loss moduli on extrudability. In this study, a higher loss tangent was shown to improve extrusion uniformity while a lower loss tangent was shown to improve structural integrity. While the ideal loss tangent window found for different gelatin-alginate concentrations may not be the same across all other hydrogel-based bioinks, the framework presented in this study could serve for future bioink development. This would further enable the progression of improved bioinks, thereby allowing for the fabrication of more complex, cell-based, soft tissue constructs in the future.

Supplementary Material

Refer to Web version on PubMed Central for supplementary material.

Acknowledgments

This study was supported by National Institutes of Health (1P41EB023833-01).

References

1. Jakus AE, Rutz AL, Shah RN. Advancing the field of 3D biomaterial printing. Biomed Mater. 2016; 11(1):014102. [PubMed: 26752507]
2. Kim JH, Yoo JJ, Lee SJ. Three-dimensional cell-based bioprinting for soft tissue regeneration. Tissue Eng Regen Med. 2016; 13(6):647–62.
3. Moroni L, Burdick JA, Highly C, Lee SJ, Morimoto Y, Takeuchi S, et al. Biofabrication strategies for 3D in vitro models and regenerative medicine. Nat Rev Mater. 2018; 3:21–37.
4. Murphy SV, Atala A. 3D bioprinting of tissues and organs. Nature biotechnology. 2014; 32(8):773–85.
5. Kang HW, Lee SJ, Ko IK, Kengla C, Yoo JJ, Atala A. A 3D bioprinting system to produce human-scale tissue constructs with structural integrity. Nature biotechnology. 2016; 34(3):312–9.

6. Duan B, Hockaday LA, Kang KH, Butcher JT. 3D bioprinting of heterogeneous aortic valve conduits with alginate/gelatin hydrogels. J Biomed Mater Res A. 2013; 101(5):1255–64. [PubMed: 23015540]
7. Wang Z, Lee SJ, Cheng HJ, Yoo JJ, Atala A. 3D bioprinted functional and contractile cardiac tissue constructs. Acta Biomater. 2018; 70:48–56. [PubMed: 29452273]
8. Merceron TK, Burt M, Seol YJ, Kang HW, Lee SJ, Yoo JJ, et al. A 3D bioprinted complex structure for engineering the muscle-tendon unit. Biofabrication. 2015; 7(3):035003. [PubMed: 26081669]
9. Chimene D, Lennox KK, Kaunas RR, Gaharwar AK. Advanced Bioinks for 3D Printing: A Materials Science Perspective. Ann Biomed Eng. 2016; 44(6):2090–102. [PubMed: 27184494]
10. Panwar A, Tan LP. Current Status of Bioinks for Micro-Extrusion-Based 3D Bioprinting. Molecules. 2016; 21(6)
11. Rutz AL, Hyland KE, Jakus AE, Burghardt WR, Shah RN. A multimaterial bioink method for 3D printing tunable, cell-compatible hydrogels. Adv Mater. 2015; 27(9):1607–14. [PubMed: 25641220]
12. Skardal A, Devarasetty M, Kang HW, Mead I, Bishop C, Shupe T, et al. A hydrogel bioink toolkit for mimicking native tissue biochemical and mechanical properties in bioprinted tissue constructs. Acta Biomater. 2015; 25:24–34. [PubMed: 26210285]
13. Tabriz AG, Hermida MA, Leslie NR, Shu W. Three-dimensional bioprinting of complex cell laden alginate hydrogel structures. Biofabrication. 2015; 7(4):045012. [PubMed: 26689257]
14. Hockaday LA, Kang KH, Colangelo NW, Cheung PY, Duan B, Malone E, et al. Rapid 3D printing of anatomically accurate and mechanically heterogeneous aortic valve hydrogel scaffolds. Biofabrication. 2012; 4(3):035005. [PubMed: 22914604]
15. Duan B. State-of-the-Art Review of 3D Bioprinting for Cardiovascular Tissue Engineering. Ann Biomed Eng. 2017; 45(1):195–209. [PubMed: 27066785]
16. Kyle S, Jessop ZM, Al-Sabah A, Whitaker IS. 'Printability' of Candidate Biomaterials for Extrusion Based 3D Printing: State-of-the-Art. Advanced healthcare materials. 2017; 6(16)
17. Paxton N, Smolan W, Bock T, Melchels F, Groll J, Jungst T. Proposal to assess printability of bioinks for extrusion-based bioprinting and evaluation of rheological properties governing bioprintability. Biofabrication. 2017; 9(4):044107. [PubMed: 28930091]
18. Zhao Y, Li Y, Mao S, Sun W, Yao R. The influence of printing parameters on cell survival rate and printability in microextrusion-based 3D cell printing technology. Biofabrication. 2015; 7(4): 045002. [PubMed: 26523399]
19. Ouyang L, Yao R, Zhao Y, Sun W. Effect of bioink properties on printability and cell viability for 3D bioplotting of embryonic stem cells. Biofabrication. 2016; 8(3):035020. [PubMed: 27634915]
20. Malda J, Visser J, Melchels FP, Jungst T, Hennink WE, Dhert WJ, et al. 25th anniversary article: Engineering hydrogels for biofabrication. Adv Mater. 2013; 25(36):5011–28. [PubMed: 24038336]
21. Zhang K, Fu Q, Yoo J, Chen X, Chandra P, Mo X, et al. 3D bioprinting of urethra with PCL/PLCL blend and dual autologous cells in fibrin hydrogel: An in vitro evaluation of biomimetic mechanical property and cell growth environment. Acta Biomater. 2017; 50:154–64. [PubMed: 27940192]
22. Gohl J, Markstedt K, Mark A, Hakansson KMO, Gatenholm P, Edelvik F. Simulations of 3D bioprinting: predicting bioprintability of nanofibrillar inks. Biofabrication. 2018
23. Nair K, Gandhi M, Khalil S, Yan KC, Marcolongo M, Barbee K, et al. Characterization of cell viability during bioprinting processes. Biotechnol J. 2009; 4(8):1168–77. [PubMed: 19507149]
24. Rauwendaal C, , Gramann PJ, , Davis BA, , Osswald TA. Polymer Extrusion Rauwendaal C, editorCincinnati, OH: Hanswer Publications; 2013
25. Kang KH, Hockaday LA, Butcher JT. Quantitative optimization of solid freeform deposition of aqueous hydrogels. Biofabrication. 2013; 5(3):035001. [PubMed: 23636927]
26. Cheng S, Clarke EC, Bilston LE. Rheological properties of the tissues of the central nervous system: a review. Med Eng Phys. 2008; 30(10):1318–37. [PubMed: 18614386]
27. Ribeiro A, Blokzijl MM, Levato R, Visser CW, Castilho M, Hennink WE, et al. Assessing bioink shape fidelity to aid material development in 3D bioprinting. Biofabrication. 2017; 10(1):014102. [PubMed: 28976364]

28. Chung JHY, Naficy S, Yue ZL, Kapsa R, Quigley A, Moulton SE, et al. Bio-ink properties and printability for extrusion printing living cells. Biomater Sci-Uk. 2013; 1(7):763–73.

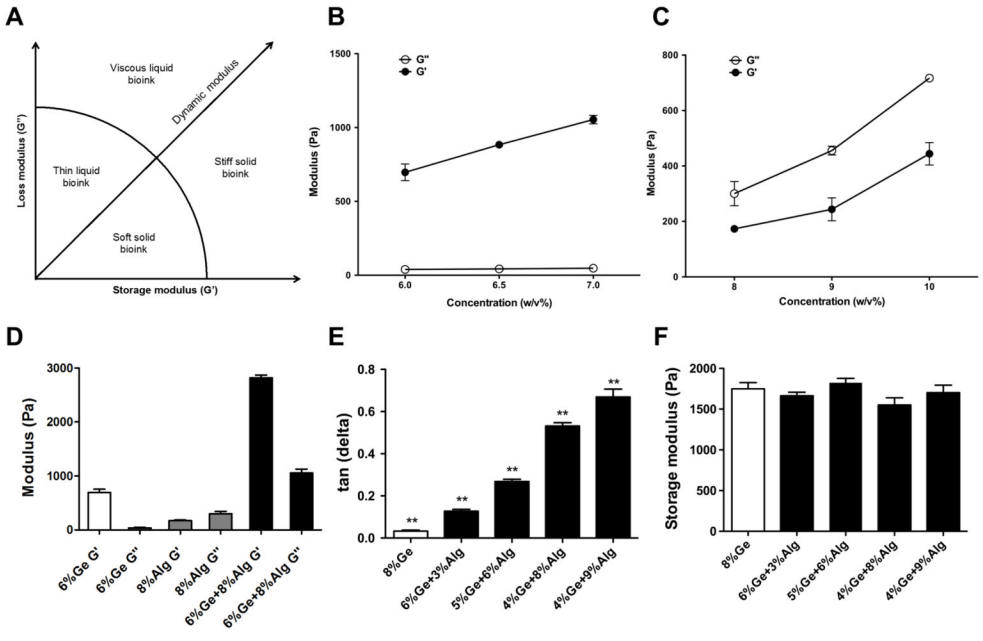

Figure 1.

Rheological measurements of common single component bioink materials. (A) Classification of common bioink materials based on storage modulus and loss modulus. (B) Rheological measurement of G' and G'' of gelatin hydrogel in three different concentrations. (C) Rheological measurement of G' and G'' of alginate hydrogel in three different concentrations. (D) Rheological measurement of G' and G'' of gelatin, alginate, and gelatin-alginate composite hydrogel. (E) Loss tangent of gelatin-alginate composite hydrogels with varying concentrations of each. (F) Storage modulus of gelatin-alginate composite hydrogels with varying concentrations of each.

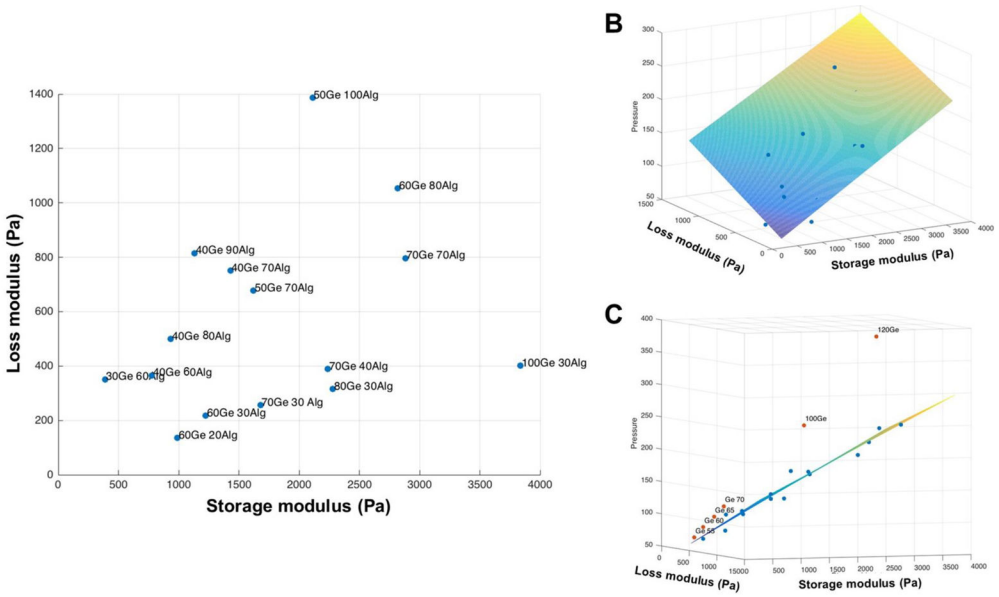

Figure 2.

(A) bioink samples used in the extrusion experiment and their rheological parameters . (B) Planer regression of extrusion pressure as a function of loss modulus and storage modulus. (C) Drop in extrusion pressure when gelatin was mixed with alginate.

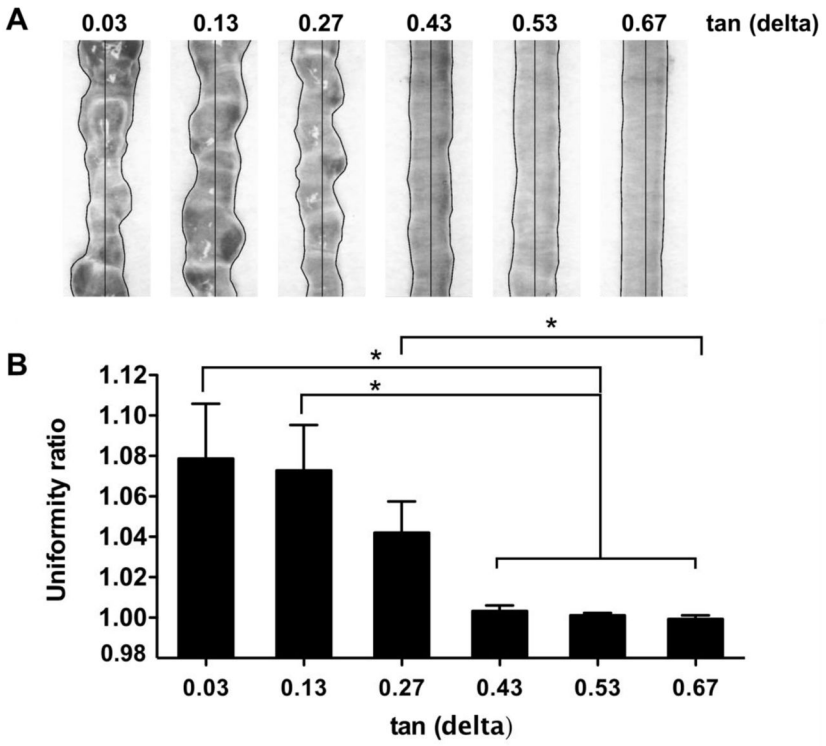

Figure 3.

Extrusion uniformity. (A) Filaments extruded from bioink samples with different loss tangent values. (B) Quantification of filament uniformity.

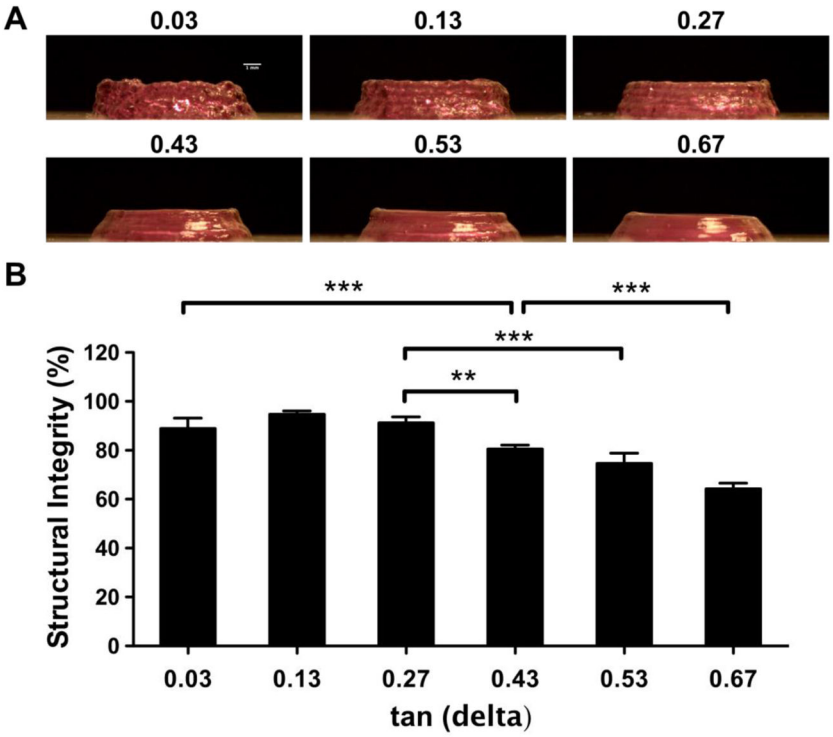

Figure 4.

Structural integrity. (A) 5-layer, cylindrical structures with different loss tangent values. (B) Quantification of structural height relative to a silicone control.

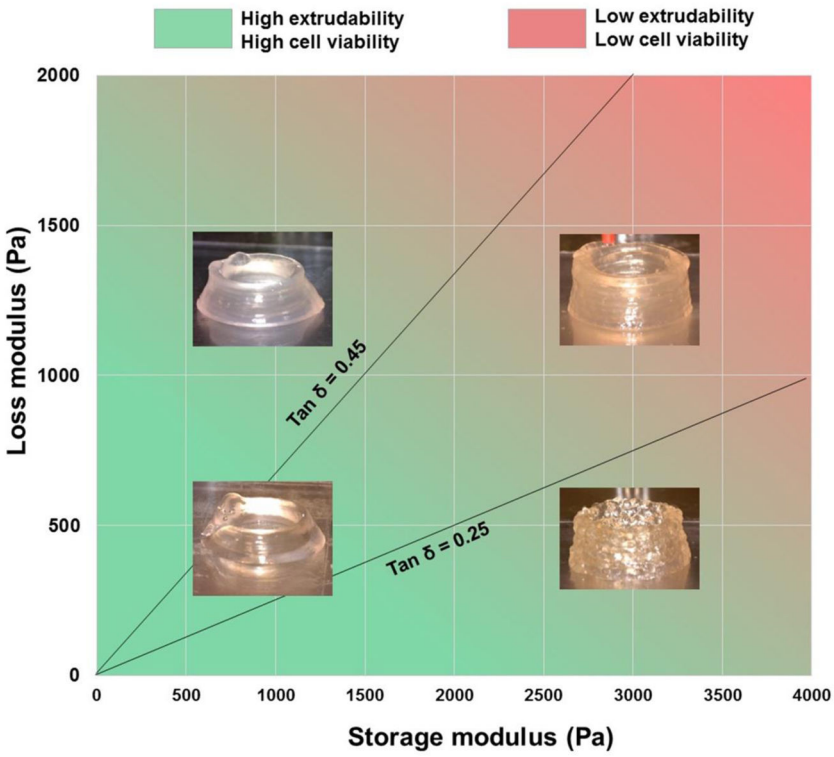

Figure 5.
Optimal region of gelatin-alginate properties for bioprinting.

Table 1

Printing parameters for experimental testing of extrusion uniformity.

Composition	Loss tangent	Pressure	Other
8%Ge	0.03	60 kPa	
6%Ge 3%Alg	0.13	70 kPa	Needle size: 25 gauge
5%Ge 6%Alg	0.27	90 kPa	Temperature: 21°C
4%Ge 7%Alg	0.43	70 kPa	Print speed: 150 mm/s
4%Ge 8%Alg	0.53	85 kPa	
4%Ge 9%Alg	0.67	70 kPa	

Ge: gelatin, Alg: alginate